Journal of Thermal Analysis and Calorimetry (2018) 133:981–989
https://doi.org/10.1007/s10973-018-7167-1

High-temperature capture of CO_2 by Li_4SiO_4 prepared with blast furnace slag and kinetic analysis

Haiyang Wang[1] · Jianliang Zhang[1] · Guangwei Wang[1] · Qi Wang[1] · Tengfei Song[1]

Received: 30 August 2017 / Accepted: 4 March 2018 / Published online: 12 March 2018

Abstract

Blast furnace slag was leached using HCl to prepare lithium-based sorbents for CO_2 capture, and chemical composition and phase of the acid leaching slag were determined by X-ray fluorescence analysis. The microstructure and morphology of both sorbents were characterized by scanning electron microscope and X-ray diffraction. The absorption capacity of both sorbents was observed non-isothermally and isothermally using thermogravimetric analysis, and 12 carbonation and calcination cycles were conducted to observe cycling stability. Controlling step of absorption process was determined by fitting the isothermal graphs using a double exponential model. The results show that 98.33% amorphous SiO_2 can be obtained when the blast furnace slag was treated at 373 K for 10 h. Purified lithium-based sorbent by acid leaching slag (LBS-ALS) shows dense polyhedral particles with particle size between 25 and 120 μm. LBS-ALS shows similar absorption capacity with pure Li_4SiO_4 (P-Li_4SiO_4), but narrower absorption temperature range at non-isothermal absorption condition. The double exponential model fits well with the isothermal graphs for LBS-ALS and P-Li_4SiO_4, and diffusion of CO_2 is the controlling step of the absorption process at lower temperature. LBS-ALS shows different controlling mechanism for desorption process compared with P-Li_4SiO_4. LBS-ALS maintains higher absorption capacity after 12 cycles in 100% CO_2 flow.

Keywords CO_2 · Blast furnace slag · Sorption · Li_4SiO_4 · Kinetic analysis

Introduction

Fossil fuel combustion has been proved to be the main reason for CO_2 emission, which contributes about 60% of the greenhouse effect [1]. China is one of the most important energy consumption countries, and coal is the main energy for the economic development now and in the future. Therefore, the rapid economic development of China in the recent years is at the cost of energy consumption and CO_2 emission, and energy conservation and emission reduction has been the most important task for China. The emission of CO_2 of iron and steel industry is approximately 4–5% of the total emission in the world according to the data by IEA [2].

The productive process of conventional iron and steel industry in China depends on fossil fuel, including coal and coke, excessively, and it has been the second emission source of CO_2 in China ranking only second to power plants [3, 4]. The crude steel production of China in 2015 exceeded 800 million tons which account for over 50% of the world. The energy consumption and CO_2 emission of iron and steel industry are 16.1 and 9.2%, respectively, and CO_2 emission is in the direct proportion to the energy consumption [5]. About 90% of the energy consumption is derived from BF-BOF process, and the energy consumption for ironmaking process is about 70% of the whole production process. Therefore, it is important for ironmaking process to reduce energy consumption and CO_2 emission in China.

CO_2 capture technology is desirable to reduce the emission of CO_2, and aqueous amine solutions and chilled ammonia have been used commercially in power plants for CO_2 separation from flue gas at low temperature [6–8]. However, the flue gas has to be cooled before separation,

---

✉ Guangwei Wang
wgw676@163.com

[1] School of Metallurgical and Ecological Engineering, University of Science and Technology Beijing, Beijing 100083, People's Republic of China

and it requires large amount of energy for the regeneration process [9]. High-temperature solid absorbents, including mainly calcium oxides and alkali metal oxides, can be used in the post-combustion process for separation of CO_2 from the flue gas. The raw material of calcium oxides is usually limestone, which is benefit to reduce the cost; however, it requires higher temperature to regenerate the calcium oxide absorbent. High absorption capacity and stable circulation property have been reported to be the most evident advantages for lithium orthosilicate, and adsorption rate, wide application temperature range and good mechanical strength properties are also the excellent performance for lithium orthosilicate [10–12].

Several authors reported the CO_2 capture in this material through the following reversible reaction [13, 14]:

$$Li_4SiO_4 + CO_2 = Li_2CO_3 + Li_2SiO_3 \quad (1)$$

The theoretical absorption capacity of lithium orthosilicate is 8.33 mmol g^{-1} according to the reaction. Investigation of synthesis methods including solid-state reactions, impregnated suspension, sol–gel method and ball milling was reported by researchers, and modification of the absorbents by doping elements, including Al, Ti, V, has been studied to resist the sinter phenomenon and enhance the performance of lithium orthosilicate. Different silica source including fly ash, rice husk ash and diatomite has been introduced to prepare lithium orthosilicate, and the results indicate that the absorption capacity is influenced by silica source obviously [15–19].

Blast furnace slag is one of the by products in iron-making process, and the main chemical composition is CaO, SiO_2, Al_2O_3 and MgO. The undelivered heat in the slag is converted into chemical energy and stored in the condition of amorphous form; therefore, the blast furnace with potential chemical activity is fine materials producing cement. Recently, the slag has been researched for high-value-added utilization. Xu et al. [20] prepared a CaO–Al_2O_3–SiO_2 system glass (MSG) from the molten blast furnace slag; the chemical composition of MSG by mass is obtained as follows: CaO 27–33%, SiO_2 42–51%, Al_2O_3 11–14%, MgO 6–8%, and $Na_2O + K_2O$ 1–4%. Kostura et al. [21] investigated the utilization of blast furnace slag as adsorbent for phosphorus in aqueous solution, and it indicates that the adsorption behavior can be explained by Langmuir adsorption isotherm. In the present study, blast furnace slag is used as silica source to prepare lithium metasilicate, acid leaching method is used to enhance silica content in the slag, and the filter liquor can be utilized to synthesis hydrotalcite-like compound according to researchers [22, 23]. Lithium metasilicate was prepared using the acid leaching slag and lithium carbonate by solid-state reaction, and pure Li_4SiO_4 was also prepared for comparison purpose. These prepared sorbents were characterized using X-ray diffraction (XRD) and scanning electron microscope (SEM), and the absorbing ability was evaluated by thermogravimetric analysis.

Experimental

Acid leaching of the blast furnace slag

The slag used in the present study is from a 3200 m^3 blast furnace in China, and the chemical composition is shown in Table 1. The slag was ground using agate mortar making the particle size less than 74 µm, and it is in favor of improving dynamic condition for acid leaching process. Concentrated hydrochloric acid with mass fraction of 36.46% was diluted to dissolve blast furnace slag. In the dilution process, 40, 45, 50 and 55 mL concentrated hydrochloric acids were diluted to 200 mL using deionized water, respectively. Ten grams pulverized blast furnace slag was dissolved in any of the diluted hydrochloric acid solution. All the mixture was heated in water bath at different temperatures for different time. The temperatures for water bath are 333, 353 and 373 K, and the heating time is 5, 10 and 15 h, respectively.

The mixture was stirred continuously to improve dynamic condition for acid leaching process. The acid leaching slag (ALS) was then filtrated and washed using deionized water many times until the pH value of filter liquor is close to 7, and then, the ALS was dried in air dry oven for 8 h.

Synthesis of Li_4SiO_4 by solid-state method

The thermodynamic parameters of the synthesis reaction were calculated using HSC, and the results are shown in Fig. 1. It indicates that gibbs free energy of the reaction decreases with increasing temperature, and the value is negative when the temperature is higher than 716.71 K indicating that the reaction can proceed at higher temperature. The reaction rate constant shows that it stays almost the same when the temperature is lower than 873 K, and it increases with increasing the reaction temperature. Therefore, the reaction temperature should be higher than 873 K.

Lithium-based sorbent from ALS (LBS-ALS) was prepared by using solid-state reaction of Li_2CO_3 (99.9%) with the ALS in a Li_2CO_3/SiO_2 mixture with molar ratio of 2.1:1. A lithium excess was added to avoid the effect of volatility of Li_2O under high temperature. The mixtures were calcined at different temperatures for different time, and the synthesis parameters are shown in Table 2. The pure Li_4SiO_4 (P-Li_4SiO_4) was prepared using chemical reagent SiO_2 (99.9%) under same condition for

Table 1 Chemical composition of the blast furnace slag

Composition	Al_2O_3	SiO_2	CaO	MgO	K_2O	Fe_2O_3	Na_2O	MnO
mass%	13.73	34.83	41.45	6.73	0.45	0.53	0.36	0.19

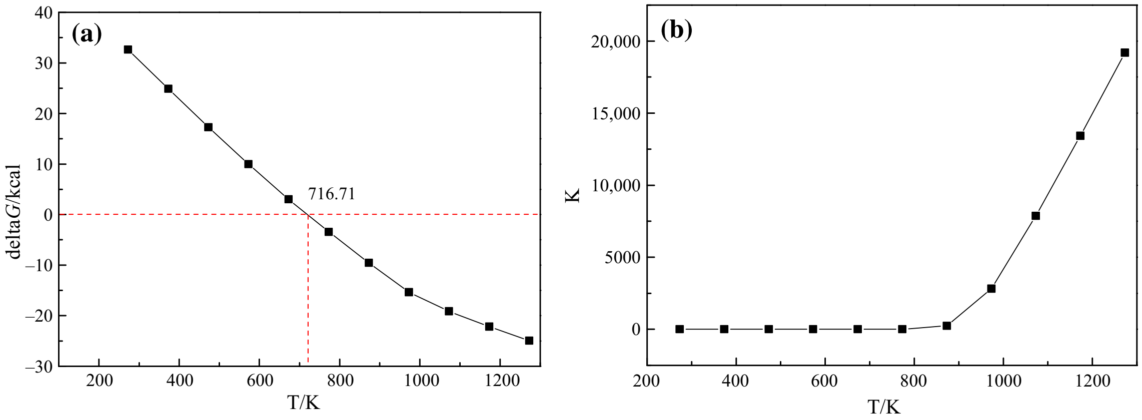

Fig. 1 Thermodynamic parameters of the synthesis reaction

Table 2 Synthesis parameters for preparing LBS-ALS

Number	Temperature/K	Time/h
1	873	4
2	873	5
3	873	6
4	973	4
5	973	5
6	973	6
7	1073	4
8	1073	5
9	1073	6

comparison. The prepared LBS-ALS was cooled in air and ground using agate mortar to crush the agglomerates.

Characterization of the sorbents

The chemical composition of the ALS was investigated by X-ray fluorometric (XRF) analysis. The microstructure and morphology of the prepared LBS-ALS were observed using a scanning electron microscope (SEM). The powder was spread uniformly onto the conductive resin surface, and the samples were coated with metal to guarantee electric conduction, and then, the samples were examined with a Quanta 250 environmental scanning electron microscopy (SEM). The LBS-ALS was dried at 378 K for 4 h, and the structural parameters were resolved using a Rigaku diffractometer, and Cu-Kα radiation (30 kV, 30 mK) was used as the X-ray source. The scanning angles were in the range from 10° to 50° (2θ) at a scan rate of 10° min^{-1}. The accelerating voltage and the applied current were 35 kV and 30 mA, respectively.

CO_2 absorption

The CO_2 absorption capacity of the LBS-ALS was determined using WCT-2 differential thermal balance produced by an optical instrument factory, Beijing, used in previous work [24]. About 10 mg sample was placed into an alumina crucible making the sample distributed uniformly. The sample was heated from room temperature to 1273 K with heating rate of 10 K min^{-1} in 100% CO_2 flow, and the gas flow is 100 mL min^{-1}. The non-isothermal analysis was conducted to find out sorption and desorption characteristics of the sorbents.

Isothermal analysis was proceeded at 873, 923, 973 and 1023 K in 100% CO_2 flow for 4 h, and the mass change of the samples was measured by the computer. To observe the cycling stability of the sorbents, 12 carbonation and calcination cycles were conducted using the thermogravimetric analyzer. The samples were heated from room temperature to 973 K with heating rate of 10 K min^{-1} in 100% N_2, and the samples reacted with CO_2 at this temperature for 1 h. Then, the samples were heated continuously to 1173 in N_2 flow for 1-h proceeding desorption, and the samples were cooled down to room temperature for another cycle. The gas flow rate for CO_2 and N_2 was all 100 mL min^{-1} to eliminate the effect of gas flow.

Results and discussion

Acid leaching condition

Mass of ALS at different conditions is shown in Fig. 2. It indicates that the treat time and temperature have obvious effect on the acid leaching process, while the influence of the concentration of hydrochloric acid solution is lighter for comparison. As the amount of HCl increases, the mass of ALS decreases, and when it is higher than 45 mL, the mass keeps almost invariant. The mass of ALS decreases from 4.63 g to 3.48 g with increasing the treat time from 5 h to 10 h at 373 K, and it keeps invariant after 10 h. Temperature has the most important influence on the acid leaching process. As temperature increases, the mass of ALS decreases obviously, and the mass is 3.37 g at 100 °C for 10 h.

The chemical composition of the ALS is shown in Table 3, and it can be seen that the content of SiO_2 is as high as 98.33% treated at 373 K for 10 h. Other compositions in the treated slag include TiO_2, Fe_2O_3, Al_2O_3, CaO and K_2O; however, the content of these compositions is all less than 1%. Therefore, the acid leaching slag can be used as silica source to prepare Li_4SiO_4.

Table 3 Chemical composition of the ALS

Composition	SiO_2	TiO_2	Fe_2O_3	Al_2O_3	CaO	K_2O
Content/%	98.33	0.65	0.28	0.23	0.09	0.01

The XRD pattern of the ALS is shown in Fig. 3, and it indicates that the ALS contains mainly SiO_2 with small amounts of trace elements, which is consistent with the result of XRF. In addition, the ALS presents a broad peak appearing around $2\theta = 22°$, which clearly indicates that it mainly consists of an amorphous silica [25].

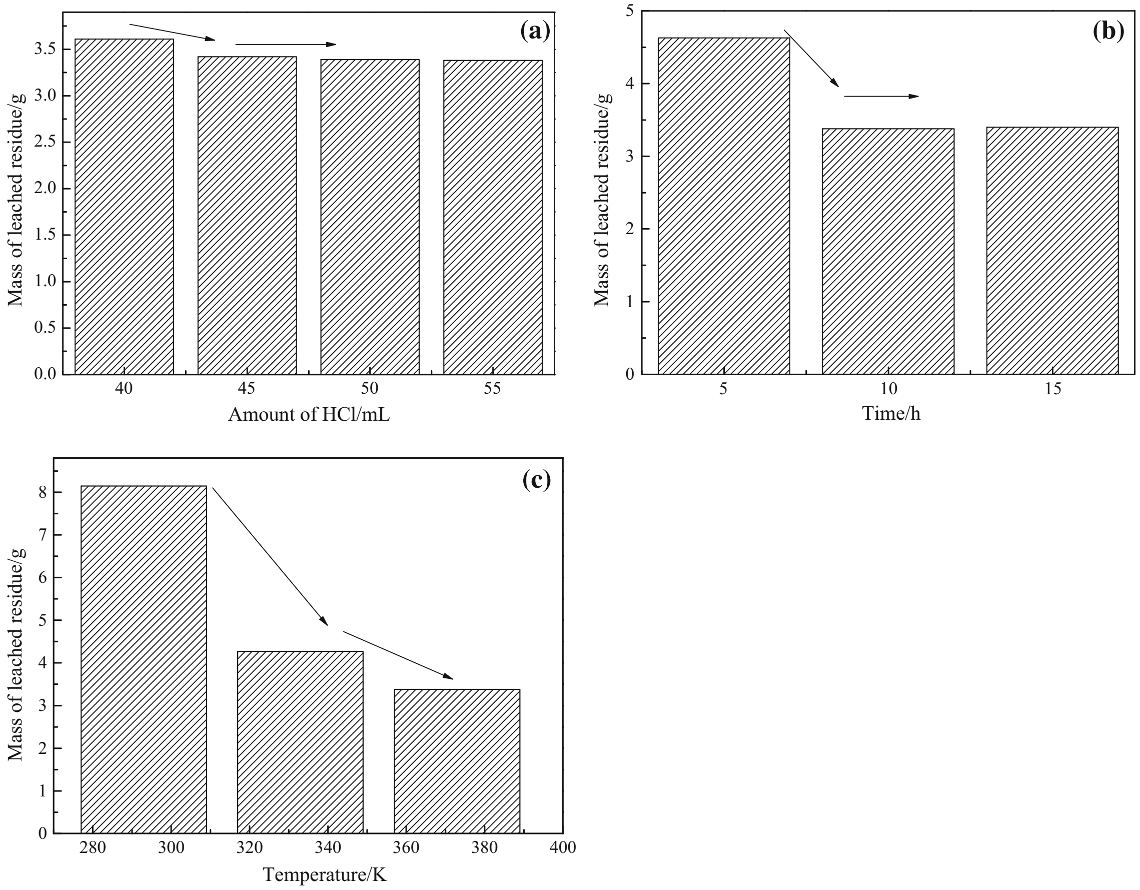

Fig. 2 Mass of ALS at different leaching conditions. **a** The slag was treated at 373 K for 5 h. **b** The slag was treated at 373 K using 50 mL concentrated hydrochloric acid diluted to 200 mL solution. **c** The slag was treated for 10 h using 50 mL concentrated hydrochloric acid diluted to 200 mL solution

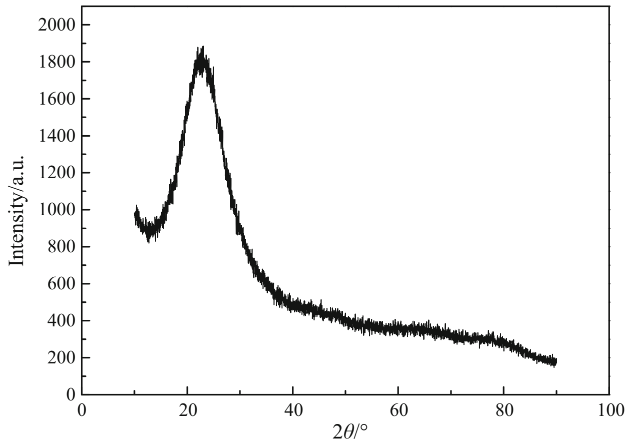

Fig. 3 XRD pattern of acid leaching slag

XRD patterns of the sorbents

Effect of preparation temperature

Figure 4 is the XRD patterns for LBS-ALS prepared with ALS at different temperatures. It indicates that temperature has a great effect on the phase composition of the sorbents. Although it can be reacted at 873 K due to thermodynamic calculation, Li_2CO_3 is still the main phase and there is only a small amount of Li_4SiO_4. In addition, Li_2SiO_3 and $Li_2Si_2O_7$ exist in the sorbents for 873 K. However, when the temperature increases to 973 K, Li_4SiO_4 becomes the main phase instead of Li_2CO_3 indicating the reaction proceeds well in this condition. At 1073 K, the content of Li_4SiO_4 increases and only trace Li_2CO_3 exists due to excess agent before calcination. It indicates that 1073 K is an optimum temperature for preparation LBS-ALS by solid-state method, which is consistent with other researches [16].

Effect of treat time

The effect of treat time on the XRD pattern is shown in Fig. 5, and it indicates that the LBS-ALS prepared at 1073 K for 4 h or 5 h contains trace content of Li_2CO_3, although the main phase is Li_4SiO_4. However, when the treat time is prolonged to 6 h, the Li_2CO_3 phase ($2\theta = 22.5°$) disappears, indicating a complete reaction between SiO_2 and Li_2CO_3.

Diffraction pattern of lithium–sodium orthosilicate and lithium–potassium orthosilicate is not observed in Figs. 4 and 5 due to the trace content in the acid leaching slag; in addition, some alkali metals are lost during calcination at 1073 K due to lower boiling point.

Figure 6 shows the comparison of the XRD profiles of P-Li_4SiO_4 with that of the LBS-ALS from ALS. The trace content of metal impurities in ALS did not modify the XRD pattern of Li_4SiO_4 phase; however, it indicates a reduction in the intensity consistent with the result by Wang et al. [26]. According to Mejía-Trejo, the solubility limit of sodium and potassium in Li_4SiO_4 is 0.1 [27]; however, Li_3NaSiO_4 and Li_2KSiO_4 are not present in both P-Li_4SiO_4 and LBS-ALS due to trace content of K_2O and Na_2O compared with the resolution of XRD.

Morphology of the sorbents

The result of XRD indicates that 1073 K is the optimum temperature for the preparation of the sorbents, and the morphology of LBS-ALS prepared at 1073 K for different time is shown in Fig. 7. The sorbents show dense polyhedral particles with particle size between 25 and 120 μm. The particles show no agglomerations when calcinated for 4 h; however, it shows agglomerates for 5 and 6 h, and the

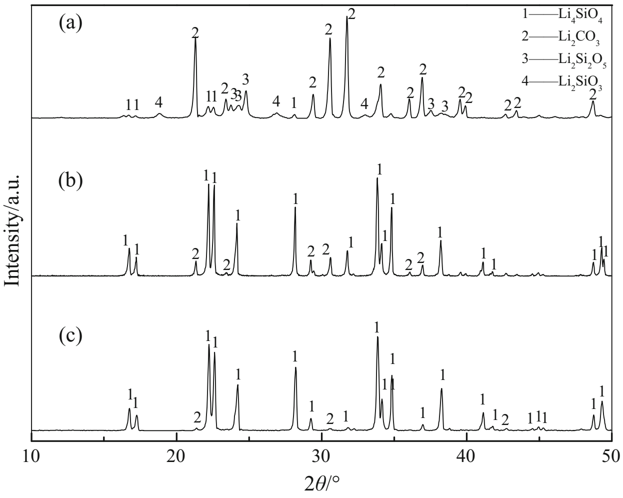

Fig. 4 Lithium-based sorbents prepared at different temperatures for 4 h. *a* prepared at 873 K; *b* prepared at 973 K; *c* prepared at 1073 K

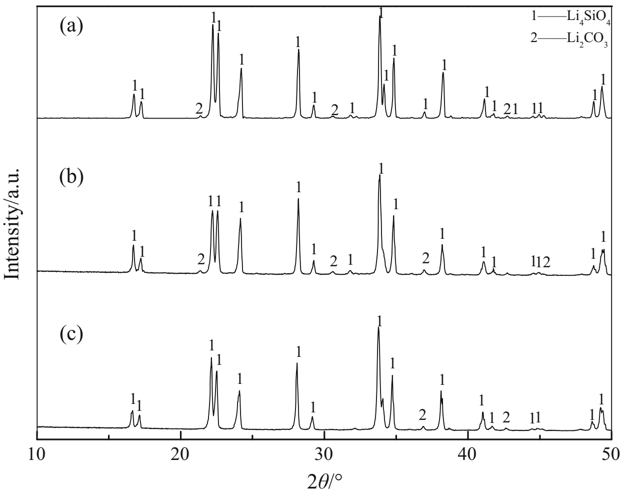

Fig. 5 Lithium-based sorbents prepared at 1073 K for different time. *a* Calcinated for 4 h; *b* calcinated for 5 h; *c* calcinated for 6 h

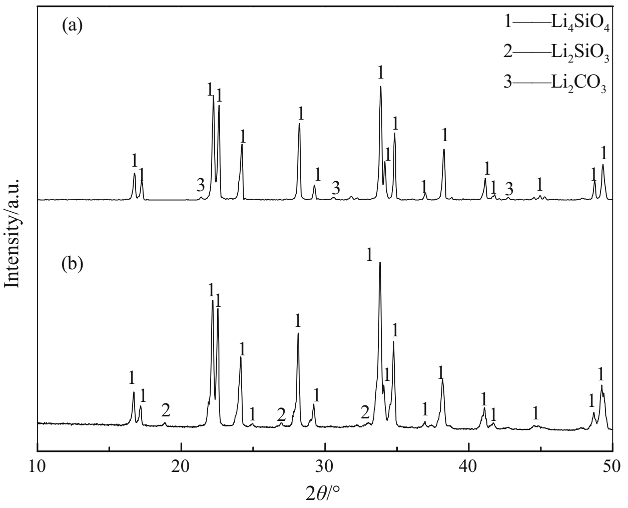

Fig. 6 Lithium-based sorbents prepared with different silica source. *a* Sorbents prepared using ALS; *b* sorbents prepared using reagent SiO_2

melt appears on the surface of the sorbents treated for 6 h. The agglomeration is related to the content of metal impurities and duration treated at high temperature according to other researchers [28, 29].

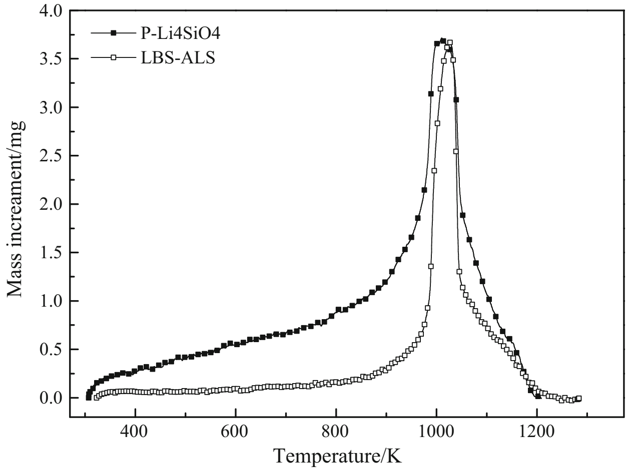

Fig. 8 Non-isothermal graphs of P-Li_4SiO_4 sorbent and LBS-ALS

CO_2 sorption capacity

Figure 8 shows the non-isothermal thermographs of the pure sorbent and that prepared by ALS and lithium carbonation. The pure sorbent captures CO_2 as soon as it contacts at low temperature, the mass of pure sorbent increases gradually until 1010.67 K, and then, it loses mass due to desorption under high temperature. However, the LBS-ALS does not absorb any CO_2 until about 773 K. The

Fig. 7 The morphology of sorbents prepared at 1073 K for different time. **a**–**c** Calcinated for 4 h; **d**–**f** calcinated for 5 h; **g**–**i** calcinated for 6 h

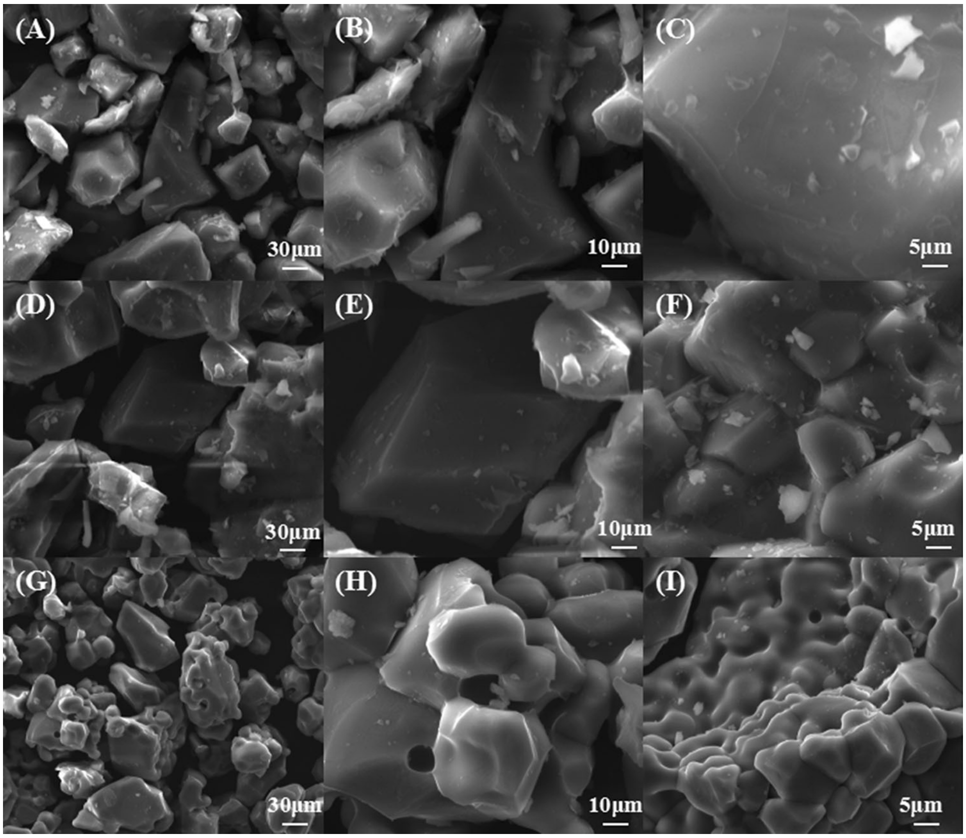

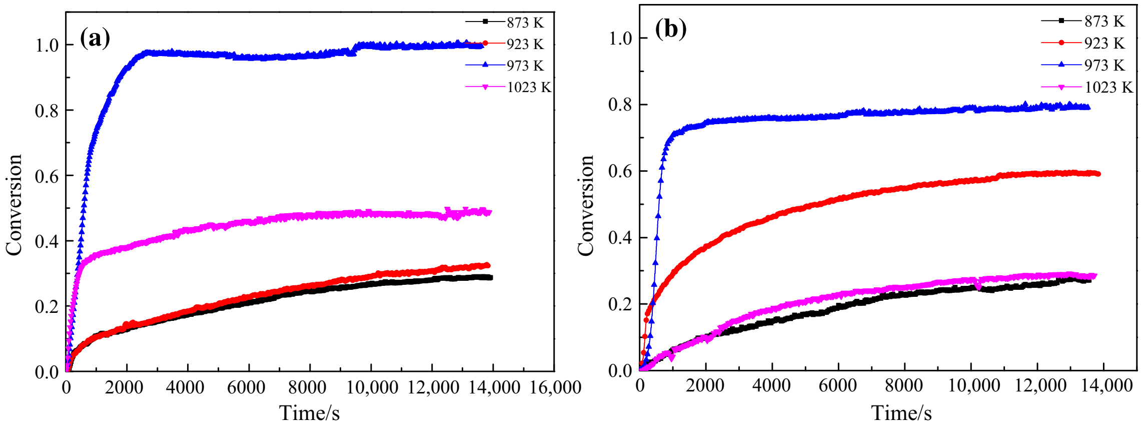

Fig. 9 Performance of sorbents prepared at 1073 K for 4 h. **a** Lithium-based sorbents; **b** pure Li_4SiO_4

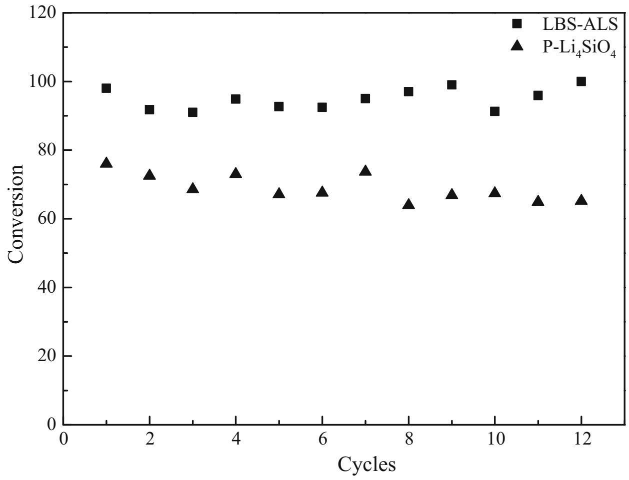

Fig. 10 Multiple cycles of sorption and desorption for both sorbents

sorbent gains mass gradually between 773 K and approximate 983 K, and it reacts with CO_2 sharply then. The mass increment increases from 0.92 to 3.65 mg only in about 4 min, and then, it decreases down to 1.30 mg in no more than 2 min. Compared with P-Li_4SiO_4 sorbent, the sorbent by ALS has narrower reaction temperature range being beneficial to energy conservation.

The isotherms at different temperatures of P-Li_4SiO_4 sorbent and LBS-ALS are shown in Fig. 9. As expected, the CO_2 adsorption capacity of both the sorbents increases as a function of temperature. After 4 h, the conversion of LBS-ALS and P-Li_4SiO_4 sorbent is 28% and 27% at 873 K, respectively. The adsorption capacity of LBS-ALS does not increase at 923 K; however, it increases to 59% for the pure sorbent. At 973 K, the conversion of LBS-ALS and the pure sorbent is 98 and 76%, respectively. It indicates an increment of adsorption capacity for the LBS-ALS due to small amount of potassium and calcium and impure phase in P-Li_4SiO_4, which is in agreement with previous reports [27]. The conversion of the sorbents decreases sharply at 1023 K, which is consistent with the non-isothermal analysis due to desorption process at high temperature.

Twelve CO_2 sorption and desorption cycles were carried out to investigate the working cyclic capacity and stability for both P-Li_4SiO_4 and LBS-ALS, and the results are

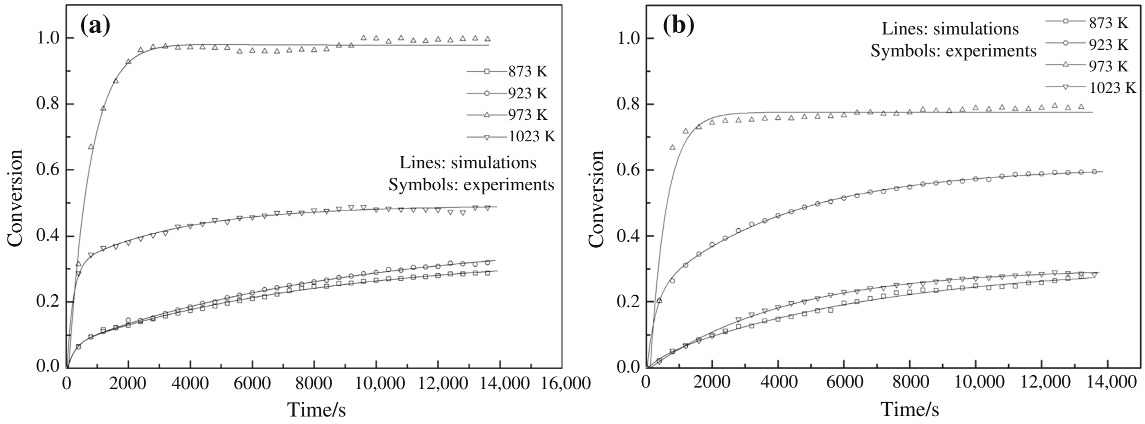

Fig. 11 Fitting results of isothermal graphs using double exponential model

Table 4 Calculation results of parameters in double exponential model

	T(K)	A	B	C	k_1	k_2	R^2
LBS-ALS	873	− 0.088	− 0.272	0.343	4.06×10^{-3}	1.23×10^{-4}	0.998
	923	− 0.08	− 0.329	0.398	3.92×10^{-3}	1.09×10^{-4}	0.992
	973	− 34.406	− 33.321	0.979	1.14×10^{-3}	1.13×10^{-3}	0.993
	1023	− 0.351	− 0.185	0.492	5.09×10^{-3}	2.77×10^{-4}	0.990
P-Li_4SiO_4	873	− 0.028	− 0.291	0.315	1.95×10^{-3}	1.43×10^{-4}	0.995
	923	− 0.244	− 0.390	0.609	3.8×10^{-3}	2.41×10^{-4}	0.998
	973	− 0.568	− 0.429	0.775	2.02×10^{-3}	2.02×10^{-3}	0.950
	1023	− 0.154	− 0.155	0.301	2.38×10^{-4}	2.38×10^{-4}	0.996

shown in Fig. 10. It indicates that the sorption capacity of LBS-ALS is higher than that of pure sorbent due to smaller particle size and metal impurities. The sorption capacity of both the sorbents remains almost unchanged even after 12 cycles indicating excellent stability. Therefore, LBS-ALS may be a new option for CO_2 absorption.

Kinetic analysis

The reaction of the sorbents with CO_2 is typical gas–solid multiple phase reaction, and the reaction process can be approximately divided mainly into two steps according to previous reports [8, 16, 27]. The CO_2 reacts with the lithium-based sorbent on the surface as soon as it contacts, and the production layer of lithium carbonation and lithium metasilicate is generated then. At the second stage, CO_2 diffuses through the layer to reach the reaction interface and reacts with each other. Therefore, a double exponential model was introduced to calculate kinetic parameters of the absorption process [16, 27]. The model can be described as:

$$y = A\exp(-k_1 t) + B\exp(-k_2 t) + C \tag{2}$$

where y is the mass increment of the sorbents, %, t is reaction time, s, k_1 and k_2 are reaction rate constants for chemisorption on the surface and chemisorption controlled by diffusion, A and B are pre-exponential factors, and C is a constant.

Nonlinear fitting method is used to calculate the parameters according to the isothermal graphs in Fig. 9. The fitting results are shown in Fig. 11, and the calculated parameters are shown in Table 4. It is obvious that the double exponential model can be used to describe the conversion of the sorbents well, and R^2 of all conditions is higher than 0.95. It indicates that k_1 values are at least 1 order of magnitude higher than those of k_2 at 873 and 923 K for both sorbents, revealing that the limiting step in the sorption process at these temperatures is diffusion of CO_2 and Li^+, and it is constant with the previous study [8]. At 973 K, indicating the reaction is controlled by both interface reaction and diffusion at this temperature. Desorption process is observed at 1023 K obviously, and k_1 value is approximately equal to that of k_2 for P-Li_4SiO_4; however, k_1 value is about 20 times higher than that of k_2 for LBS-ALS indicating different controlling mechanism for desorption process.

Conclusions

Silica source can be derived from blast furnace slag to prepare highly efficient sorbent for CO_2 capture. When the blast furnace slag was treated at 373 K for 10 h using 45 mL HCl diluted to 200 mL, the content of amorphous SiO_2 was 98.33%. Highly purified LBS-ALS can be synthesized at 1023 K for 4 h, and the particle size is smaller than that of P-Li_4SiO_4 due to metal impurities. LBS-ALS shows similar absorption capacity with P-Li_4SiO_4, but narrower absorption temperature range at non-isothermal absorption condition. However, the absorption capacity of LBS-ALS is different from that of P-Li_4SiO_4, and the conversion of LBS-ALS is 98% at 973 K, which is higher than P-Li_4SiO_4 due to smaller particle size and impurities. LBS-ALS maintains higher absorption capacity after 12 carbonation/calcination cycles. The double exponential model fits well with the isothermal graphs for both sorbents showing chemical reaction and diffusion mechanism. Diffusion process is the controlling step at lower temperature, and mixed control of interface reaction and diffusion takes place at 973 K. In addition, LBS-ALS shows diffusion-controlled mechanism in desorption process; however, it is mixed control for P-Li_4SiO_4.

Acknowledgements The present work was supported by National Key Technology R&D Program (No. 2011BAC01B02).

References

1. VandenBerg AWC, Arean CO. Materials for hydrogen storage: current research trends and perspectives. Chem Commun. 2008;2008:668–81.
2. IEA. Energy technology perspectives 2010-scenarios and strategies to 2050, Paris, France; 2010. pp. 650–656.
3. Huitu K, Helle H, Helle M, et al. Optimization of steel making using fastmet direct reduced iron in the blast furnace. ISIJ Int. 2003;53:2038–46.
4. Dhunna R, Khanna R, Mansuri I, et al. Recycling waste bakelite as an alternative carbon resource for ironmaking applications. ISIJ Int. 2014;54:613–9.
5. Rui R, Duan W. Current situation of CO_2 emission in iron and steel producing and its controlling methods. Sci Technol Rev. 2016;24:53–6.
6. Kittel J, Idem R, Gelowitz D, et al. Corrosion in MEA units for CO_2 capture: pilot plant studies. Energy Proc. 2009;1:791–7.
7. McLarnon CR, Duncan JL. Testing of ammonia based CO_2 capture with multi-pollutant control technology. Energy Proc. 2009;1:1027–34.
8. Wang X, Alvarado V, Swoboda-Colberg N, et al. Reactivity of dolomite in water-saturated supercritical carbon dioxide: significance for carbon capture and storage and for enhanced oil and gas recovery. Energy Convers Manage. 2013;65:564–73.
9. Pennline HW, Luebke DR, Jones KL, et al. Progress in carbon dioxide capture and separation research for gasification-based power generation point sources. Fuel Process Technol. 2008;89:897–907.
10. Gauer C, Heschel W. Doped lithium orthosilicate for absorption of carbon dioxide. J Mater Sci. 2006;41:2405–9.
11. Nakagawa K, Essaki K. CO_2 absorption by lithium silicate at room temperature. J Chem Eng Jpn. 2004;6:772–90.
12. Bretado ME, Velderrain VG, Gutiérrez DL, et al. A new synthesis route to Li_4SiO_4 as CO_2 catalytic/sorbent. Catal Today. 2005;107:863–7.
13. Nair BN, Burwood RP, Goh VJ, et al. Lithium based ceramic materials and membranes for high temperature CO_2 separation. Prog Mater Sci. 2009;54:511–41.
14. Chowdhury MBI, Quddus MR, DeLasa HI. CO_2 capture with a novel solid fluidizable sorbent: thermodynamics and temperature programmed carbonation–decarbonation. Chem Eng J. 2017;232:139–48.
15. Olivares-Marín M, Drage TC, Maroto-Valer MM. Novel lithium-based sorbents from fly ashes for CO_2 capture at high temperatures. Int J Greenh Gas Control. 2010;4:623–9.
16. Venegas MJ, Fregoso-Israel E, Escamilla R, et al. Kinetic and reaction mechanism of CO_2 sorption on Li_4SiO_4: study of the particle size effect. Ind Eng Chem Res. 2007;46:2407–12.
17. Ortiz-Landeros J, Gómez-Yáñez C, Palacios-Romero LM, et al. Structural and thermochemical chemisorption of CO_2 on $Li_{4+-x}(Si_{1-x}Al_x)O_4$ and Li_{4-x} $(Si_{1-x}V_x)O_4$ solid solutions. J Phys Chem. 2012;116:3163–71.
18. Ni J, Kawabe Y, Morishita M, et al. Improved electrochemical activity of $LiMnPO_4$ by high-energy ball-milling. J Power Sources. 2011;196:8104–9.
19. Romero-Ibarra IC, Jortiz-Landeros J, Pfeiffer H. Microstructural and CO_2 chemisorption analyses of Li_4SiO_4: effect of surface modification by the ball milling process. Thermochim Acta. 2013;567:118–24.
20. Xu Y, Zhang YZ, Hou LY, et al. Preparation of $CaO–Al_2O_3–SiO_2$ system glass from molten blast furnace slag. Int J Min Metals Mater. 2014;21:169–74.
21. Kostura B, Kulveitová H, Leško J. Blast furnace slags as sorbents of phosphate from water solutions. Water Res. 2005;39:1795–802.
22. Adachi-Pagano M, Forano C. Synthesis of Al-rich hydrotalcite-like compounds by using the urea hydrolysis reaction?control of size and morphology. J Mater Chem. 2003;13:1988–92.
23. Li DL, Koike M, Chen JH, et al. Preparation of Ni–Cu/Mg/Al catalysts from hydrotalcite-like compounds for hydrogen production by steam reforming of biomass tar. Int J Hydrog Energy. 2014;39:10959–70.
24. Wang HY, Zhang JL, Wang GW, et al. Characteristics and kinetic analysis of co-combustion of brown coal and anthracite. J Therm Anal Calorim. 2016;126:447–54.
25. Feng Q, Lin Q, Gong F, et al. Adsorption of lead and mercury by rice husk ash. J Colloid Interface Sci. 2004;278:1–8.
26. Wang K, Guo X, Zhao P, et al. High temperature capture of CO_2 on lithium-based sorbents from rice husk ash. J Hazard Mater. 2011;189:301–7.
27. Victoria L, Mejía-Trejo E, Fregoso-Israel H. Textural, structural, and CO_2 chemisorption effects produced on the lithium orthosilicate by its doping with sodium($Li_{4-x}Na_xSiO_4$). Chem Mater. 2008;20:7171–6.
28. Liu W, Feng B, Wu Y, et al. Synthesis of sintering-resistant sorbents for CO_2 capture. Environ Sci Technol. 2010;44:3093–7.
29. Steenari BM, Lindqvist O. High temperature reactions of straw ash and the anti-sintering additives kaolin and dolomite. Biomass Bioenergy. 1998;14:67–76.